Constrained Optimization for Disoccluding Geographic Landmarks in 3D Urban Maps

Daichi Hirono * Hsiang-Yun Wu † Masatoshi Arikawa ‡ Shigeo Takahashi §

The University of Tokyo

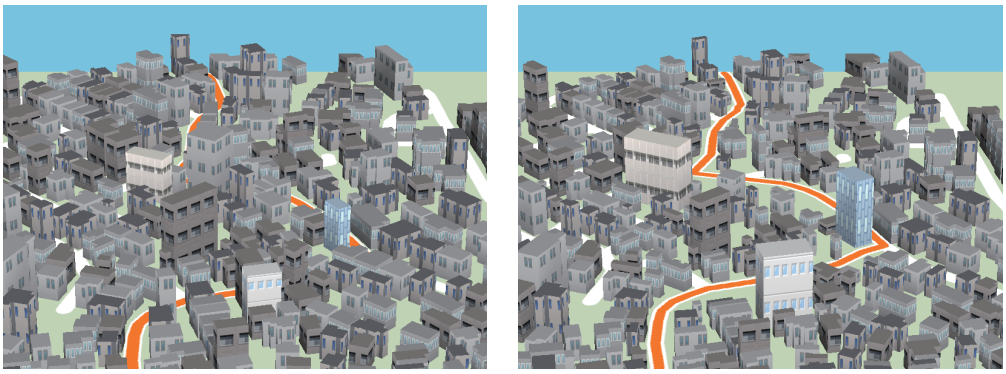

Figure 1: Side-by-side comparison between an ordinary perspective view (left) and its optimally distorted version with our approach (right). Note that we can successfully avoid the occlusions of important route to the destination (drawn in orange) while accentuating the 3D appearance of the landmark buildings. (Kikuna, Yokohama, Japan.)

ABSTRACT

In composing hand-drawn 3D urban maps, the most common design problem is to avoid overlaps between geographic features such as roads and buildings by displacing them consistently over the map domain. Nonetheless, automating this map design process is still a challenging task because we have to maximally retain the 3D depth perception inherent in pairs of parallel lines embedded in the original layout of such geographic features. This paper presents a novel approach to disoccluding important geographic features when creating 3D urban maps for enhancing their visual readability. This is accomplished by formulating the design criteria as a constrained optimization problem based on the linear programming approach. Our mathematical formulation allows us to systematically eliminate occlusions of landmark roads and buildings, and further controls the degree of local 3D map deformation by devising an objective function to be minimized. Various design examples together with a user study are presented to demonstrate the robustness and feasibility of the proposed approach.

Index Terms: I.3.8 [Computer Graphics]: Applications;

1 INTRODUCTION

When visualizing urban environments, 3D perspective views are usually preferable to 2D top views in the sense that they provide depth information and thus yield a better visual matching with real landscapes we see in our daily life. Such 3D representation of urban environments has already been common in car navigation systems, and is now becoming popular for browsing maps on mobile devices due to the development of graphics hardware. This naturally leads us to an important technical problem of improving the visual readability of such 3D urban maps.

For enhancing such map readability, we can identify common *design criteria* often employed in hand-drawn illustrative maps created by *cartographic* artists. As shown in Figure 2, one of the major criteria is to apply appropriate deformation to the 3D urban map so that we can avoid *occlusions* of important geographic features including important routes and landmark buildings. Nonetheless, it is still a challenging issue to disocclude such important geographic features while preserving the global layout of the 3D map. This will be much harder especially when visualizing 3D urban environments since each road in the urban area is more likely to be occluded by high buildings in its neighborhood. Furthermore, we usually have to control the orientation of parallel lines inherent in the arrangement of roads and shapes of 3D buildings for retaining the associated 3D *depth cues*. Note that we still suffer from this occlusion problem simply by employing *translucent* representations of the 3D map content since we cannot fully retrieve the depth information of each geographic feature when it overlaps with other objects an excessive number of times.

This paper presents an approach to automatically disoccluding important geographic features in 3D urban map visualization. This is accomplished by finding an appropriate deformation to the 3D map geometry in the sense that we can avoid occlusions of such important features while faithfully retaining their relative positions together with the associated depth, including pairs of parallel lines that outline artificial geographic features. Our technical contribution lies in formulating this problem as a *constrained optimization problem*, where we encode several design criteria of 3D urban maps as linear constraints and optimize the associated map deformation using *linear programming* techniques. Figure 1 shows a side-by-side comparison between an original 3D urban map and its optimized version, which demonstrates how we can successfully avoid

*e-mail: hirono@visual.k.u-tokyo.ac.jp
†e-mail: yun@visual.k.u-tokyo.ac.jp
‡e-mail: arikawa@csis.u-tokyo.ac.jp
§e-mail: takahashis@acm.org

Figure 2: An example of a hand-drawn illustrative map of Tokyo, Japan (courtesy of WORKS-PRESS CO., LTD.).

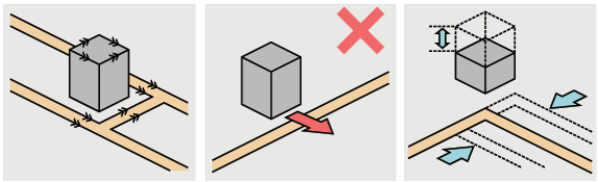

(a) Fixed orientation (b) Relative position (c) Scale limits

(d) Minimum displacement (e) Occlusion avoidance

Figure 3: Five design criteria.

overlaps between the route to the destination and its surrounding buildings using our approach.

Unlike conventional approaches, we can provide a fully automatic algorithm for optimizing such map deformation to disocclude landmark features since the cost function together with its associated constraints has been explicitly defined. Furthermore, our new formulation introduces more degrees of freedom into the map deformation so as to simulate the skills of cartographic artists as shown in Figure 2. The proposed approach also differs in that it can discover *practically feasible* solutions even in *unsolvable* cases, by incorporating into the constrained optimization a new cost term that penalizes the occlusions of such geographic features. In practice, this enables us to adjust the final optimized layout of 3D urban maps by assigning different weights to the deformation and penalty cost terms. (See Figure 12 for an example.)

The remainder of this paper is organized as follows. Section 2 provides a survey on previous methods. Section 3 describes design criteria we introduce for disoccluding geographic features in 3D urban maps. Section 4 presents how we can formulate such design criteria as a constrained optimization problem, which is followed by several enhancements in Section 5. After having provided design examples and results of a user study in Section 6, Section 7 concludes this paper and refers to possible extensions of this work.

2 Related Work

For automating map design, it is often important to simulate cartographic techniques commonly used in conventional hand-drawn maps [14]. Agrawala and Stolte [1] presented an effective approach for generating *route-aware maps* by generalizing such cartographic styles. This idea was further enhanced by the work of Kopf et al. [10], where they also incorporated the road networks around the primary route so that users can identify its relative position.

Focus+context techniques make it possible for us to interactively explore the map contents according to our preferences. Distortion-oriented presentation is a commonly used technique for providing the detailed view of some specific region [11]. Carpendale et al. [2] achieved higher magnification in focus+context previews and demonstrated its efficiency in exploring the details of 2D map contents. This line of research has been further improved by graph-based optimization techniques to enlarge user-defined focus regions on schematic metro maps [22] and road networks [9]. Trapp et al. extended such focus+context visualization strategies to cover 3D virtual city models [21] and its enhanced version with different abstraction levels [18]. An interesting variation was also proposed by Chaudhuri and Shen [3], where they created extra screen space for providing additional information in 3D space while minimizing occlusion of the underlying 2D map.

Disoccluding important geographic landmarks from their surrounding objects is another important way to improve the readability of the 3D map representations [13]. Takahashi et al. [19] first presented occlusion-free representation of routes specifically in *mountain* areas and its animation for application to car navigation systems. This work has been followed by an approach by Möser et al. [15], where they distorted the terrain surface to be aligned with the predefined base surface to reduce possible occlusions of geographic features. Degener and Klein [6] constructed a variational formulation for automating occlusion-free representation of ski and hiking courses in mountain areas. Cui et al. [5] implemented GPU-accelerated techniques for occlusion-free visualization and demonstrated real-time navigation in canyon terrain areas.

Avoiding occlusion of geographic landmarks is further involved especially in the visualization of 3D *urban* environments. This is because the scene usually contains many depth cues such as pairs of parallel lines arising from roads in parallel and building silhouettes, and thus we have to limit the distortion of 3D map geometry for preserving the associated depth information. Grabler et al. [8] introduced displacement, scaling, and removal of buildings within each urban block to avoid occlusions of surrounding roads to increase the visual readability of the 3D urban maps. Qu et al. [17] presented the most relevant work to ours, where they sophisticated a seam carving algorithm to appropriately partition the 2D map domain and spared additional space along the seams running on specific roads through a grid-based zooming technique [23]. Liqiang et al. [12] proposed a different segmentation technique by constructing a proximity graph for grouping buildings and inserting additional space between the building clusters. Readers can refer to [7] for further details on occlusion management in 3D visualization.

Our approach shares with conventional algorithms the idea of displacing roads and buildings and lowering the building heights in order to avoid occlusions of important geographic landmarks. Nonetheless, the proposed approach differs in that it explicitly quantifies such spatial displacement of geographic features as a cost and optimizes it under the constraints derived from map design criteria. Such constraint-based approaches have been applied to graph drawing problems [20] and 3D camera control [4]. Indeed, this mathematical formulation allows us to automatically optimize the map deformation, and thus requires minimal user intervention for finding visually plausible layouts of 3D urban maps.

3 Design Criteria for 3D Urban Maps

We first establish design criteria for occlusion-free representation of landmarks in our 3D urban maps. Actually, we have learned common *functional aesthetics* from observation of hand-drawn illustrative maps (e.g. Figure 2), and decided to employ the following five design criteria for improving the map readability.

Fixed orientation (Figure 3(a)): We should faithfully preserve the orientations of paired parallel lines because they usually con-

stitute the silhouette of artificial geographic features such as roads and buildings and thus their orientations should be consistent with each other to avoid unnatural depth cues in the finalized map layout.

Relative position (Figure 3(b)): The relative position of each geographic feature with respect to its adjacent features must be retained over the 2D map domain. In particular, we are prohibited to swap them to maintain the global context of the map layout.

Scale limits (Figure 3(c)): It is important to restrict the changes in the horizontal and vertical scales of each geographic objects, respectively, within predefined ranges, since drastic changes in individual geographic objects will result in visual artifacts.

Minimum displacement (Figure 3(d)): The position of each geographic feature should be as close as possible to its original position, in order to maximally retain the overall appearance of the original 3D urban environments.

Occlusion avoidance (Figure 3(e)): Avoiding occlusions of important landmarks caused by surrounding objects is our primary objective toward the high readability of the 3D urban maps.

Note that the first three criteria are employed for keeping the *consistency* in the arrangement of geographic features and formulated as *hard* constraints, while the last two are introduced as *soft* constraints for enhancing the reality and readability of 3D urban maps, respectively. Our challenge here is to find a deformation of 3D map geometry that suffices these five design criteria. We formulate this problem as a constrained optimization problem by employing linear programming techniques, which will be detailed in the next section.

4 Constrained Optimization Problem Formulation

As stated earlier, we find an optimal layout of the 3D urban map by solving a constrained optimization problem using the linear programming technique. Indeed, it allows us to optimize the linear combination of variables $(\xi_1,\ldots,\xi_n)$ as the objective cost function:

$$f(\xi_1,\ldots,\xi_n) = \gamma_1\xi_1 + \cdots + \gamma_n\xi_n, \tag{1}$$

on the condition that the variables $(\xi_1,\ldots,\xi_n)$ stay within the convex space confined by a set of linear inequalities:

$$\begin{cases} \alpha_{11}\xi_1 & + & \cdots & + & \alpha_{1n}\xi_n & \leq & \beta_1 \\ & & & & \vdots & & \\ \alpha_{m1}\xi_1 & + & \cdots & + & \alpha_{mn}\xi_n & \leq & \beta_m. \end{cases} \tag{2}$$

Linear programming is a classic method, while it has been still applied to recent visualization problems such as readability enhancement in parallel coordinates [24], and its integer version to schematic representation of metro maps [16]. In this section, we first describe how the geographic features such as roads and buildings are represented in our formulation. We then present how we can encode the first three hard constraints and last two soft constraints as linear constraints and objective cost terms.

4.1 Representation of geographic features

Our approach takes as inputs the coordinates of geographic features and finds their optimized positions in the final map layout as the solution of the constrained optimization problem. As the geographic features, we consider road networks and buildings where each cluster of buildings is assumed to be in a *urban block* bounded by a set of the roads. Each road is represented as a polyline consisting of a sequence of 2D point samples on the map domain while its connections with other roads are explicitly defined as a network. A building is modeled as a prism consisting of the 2D basement polygon and height. As an option, users can interactively designate a sequence of road segments and a set of buildings as landmarks in order to make such geographic features clearly pop up from the optimized layout of 3D urban maps.

We assume that the road networks and building basements are represented as a graph in our formulation, and refer to a sample point and a line segment as a *vertex* and an *edge*, respectively, in this paper. Note that, in our setting, the road networks and the basements of buildings are placed on the xy-plane that coincides with the ground surface. Furthermore, the positive y-axis is aligned with the depth direction while the positive x-axis is directed horizontally to the right accordingly. This means that a road is represented as a sequence of vertices each of which has the (x,y)-coordinates while a building is defined by the 2D planar positions of the basement corners together with its height h. In what follows, we use this notation in order to formulate the linear programming problem.

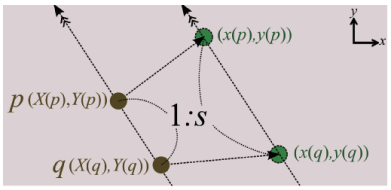

Figure 4: Fixed orientation constraint. The orientation of the edge $\overline{pq}$ is fixed while its scale ratio changes.

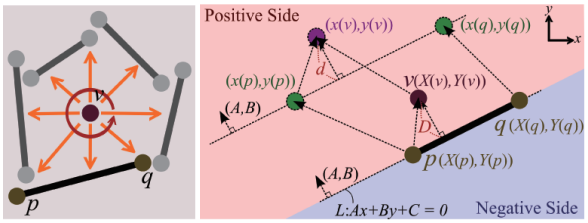

(a) (b)

Figure 5: Relative position constraint. (a) Neighbor edges that surround the vertex v. (b) The vertex v and its neighbor edge $\overline{pq}$.

4.2 Formulating hard constraints

We formulate the first three design criteria as *hard constraints*, and then introduce the corresponding set of linear equalities and inequalities into our linear programming model.

Fixed orientation The *fixed orientation* constraint is imposed on a pair of vertices that share an edge on the 2D ground plane, so that the orientation of that edge segment is fixed during the optimization process. As describe earlier, this constraint helps us maximally preserve the foreshortening effects, especially those produced by parallel lines along the roads and building silhouettes. For example, Figure 4 illustrates how we can formulate the fixed orientation constraint for the edge $\overline{pq}$. Let us denote the original 2D coordinates of p and q by $(X(p),Y(p))$ and $(X(q),Y(q))$, respectively. Since $X(p)$, $X(q)$, $Y(p)$, and $Y(q)$ are constants, the orientation of the edge $\overline{pq}$ can be preserved by the following two linear equations:

$$\begin{cases} x(p) - x(q) &= s\,(X(p) - X(q)) \\ y(p) - y(q) &= s\,(Y(p) - Y(q)) \end{cases} \tag{3}$$

Here, $(x(p),y(p))$ and $(x(q),y(q))$ are variables that denote the newly optimized coordinates of p and q, respectively, and s is another variable representing the scale ratio of the optimized edge length with respect to its original one. In our approach, we impose the above constraints on *all* the road and building basement edges.

Relative Position The *relative position* constraint is used to maintain the original spatial relationship between a vertex and its neighbor edges along the xy-plane, thus enables us to avoid unacceptable cases where the vertex goes across the edges during the optimization process. For this purpose, we collect a sufficient number of neighbor edges to surround 360 degrees around *every* vertex v on the xy-plane as a preprocess, as shown in Figure 5(a). Note that our experiments show that we extract 7 neighbor edges on average for each vertex in this preprocess. We then consider linear constraints that will be imposed on the vertex v and one of the neighbor edges $\overline{pq}$. Suppose that the equation of the line L passing through $\overline{pq}$ is given by $Ax+By+C=0$, where $A^2+B^2=1$ and $B \geq 0$ hold. Figure 5(b) shows such a case where the overall map domain is divided into the positive side ($Ax+By+C>0$) and negative side ($Ax+By+C<0$). Note that the values A, B, and C can be easily calculated from the original coordinates of p and q. For preserving the relative position of v with respect to $\overline{pq}$, we have to impose linear constraints that force v to stay within the same side. Since (A,B) is the unit normal vector of L, the signed distance D between $\overline{pq}$ and v can be represented by the inner product of the vector $\overrightarrow{pv}$ and unit normal vector (A,B), as

$$D = A(X(v)-X(p))+B(Y(v)-Y(p)). \tag{4}$$

This implies that the vertex v resides in the positive side if $D>0$ and in the negative side if $D<0$. A new distance d from $\overline{pq}$ to v after the optimization process can be obtained in the same way as

$$d = A(x(v)-x(p))+B(y(v)-y(p)), \tag{5}$$

because the orientation of $\overline{pq}$ has been preserved using the fixed orientation constraints. In our implementation, the relative position constraint is defined as

$$\begin{cases} A(x(v)-x(p))+B(y(v)-y(p)) \geq \min\{|D|,M\} & \text{if } D>0 \\ A(x(v)-x(p))+B(y(v)-y(p)) \leq -\min\{|D|,M\} & \text{if } D<0 \end{cases} \tag{6}$$

where $M(\geq 0)$ denotes a predefined small value introduced to spare the marginal space between the vertex and edge. Note that we use the value $|D|$ instead of M if the original distance between $\overline{pq}$ and v is smaller than M, which empirically prevents us from suffering from infeasible problems. In our implementation, we set M to be equivalent to the half width of a road to spare enough space between the roads and buildings.

Scale Limits The *scale limits* constraints are employed to adjust the sizes of artificial geographic features such as roads and buildings within visually acceptable ranges. We impose the constraints on the lengths of *all* the road and building basement edges and the heights of *all* the buildings, so that we can avoid unexpected distortions of individual features in the finalized map layout. In our implementation, the length of each edge is constrained by bounding its corresponding scale ratio in Eq. (3) as follows:

$$\tfrac{1}{2} \leq s \leq 2, \tag{7}$$

where these upper and lower scale limits are determined empirically. The optimized height of each building is controlled so as to keep it no less than the half of its original height, as

$$\tfrac{H}{2} \leq h \leq H, \tag{8}$$

where H corresponds to the original height of the building. This helps us avoid unnaturally short buildings in the final map layout.

4.3 Formulating soft constraints

The last two design criteria are interpreted as *soft constraints* and thus incorporated into our formulation as *cost terms* together with additional linear inequality constraints.

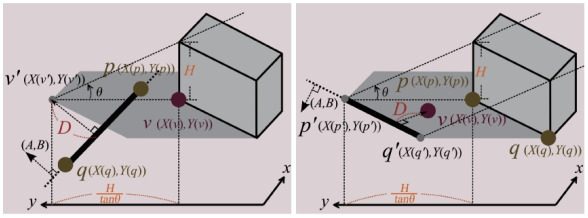

(a) (b)

Figure 6: Occlusion avoidance constraints. (a) A constraint of the first type on a building vertex v and a road edge $\overline{pq}$. (b) A constraint of the second type on a road vertex v and a building edge $\overline{pq}$.

Minimum displacement Let V_r and V_b denote the sets of road and building basement vertices, respectively. The *minimum displacement* constraint first minimizes the horizontal displacement of each vertex $v(\in V_r+V_b)$ from its original position. This is accomplished by introducing

$$\begin{cases} -\delta_x \leq x(v)-X(v) \leq \delta_x \\ -\delta_y \leq y(v)-Y(v) \leq \delta_y \end{cases} \tag{9}$$

where $\delta_x(\geq 0)$ and $\delta_y(\geq 0)$ are new variables representing the displacements of v along the x and y-axes, respectively.

We also penalize the change in the height of each building

$$H-h \tag{10}$$

where H and h denote the original and newly optimized heights of the building at $v(\in V_b)$, respectively. Thus, the cost function for the minimum displacement constraints is defined by summing up normalized horizontal and vertical displacements as

$$W_d \sum_{v \in V_r+V_b} (\delta_x+\delta_y) + W_h \sum_{v \in V_b} (H-h) \tag{11}$$

where W_d and W_h correspond to the weight values of the horizontal and vertical cost terms, respectively. Note that we penalize the 2D displacement of each vertex along the ground plane using the Manhattan distance metric in the above formulation.

Occlusion avoidance The *occlusion avoidance* constraints will allow us to disocclude important landmark roads, which may overlap with surrounding buildings in the original layout. In practice, the occlusion avoidance constraints are categorized into two types: one is for a building vertex and a road edge and the other is for a road vertex and a building edge. Note that we first consider the orthographic projection and fix its angle of elevation to be θ for simplicity in the following explanation. Extension of this formulation to perspective projection will be given later in Section 5.3.

For the first type of constraint, let us consider a road edge $\overline{pq}$ that has an intersection with the vertical building edge at the vertex v in the original layout, as shown in Figure 6(a). Assume that the top vertex of the vertical edge at v is projected onto the point v' on the xy-plane. If the building originally has the height H, we can write the (x,y)-coordinates of v' as

$$(X(v'),Y(v')) = (X(v),Y(v)+\tfrac{H}{\tan\theta}), \tag{12}$$

using the original coordinates of v $(X(v),Y(v))$, since the view line is perpendicular to the x-axis in our setting. Now suppose that the expression of the line L that contains p and q is $Ax+Bx+C=0$, where $A^2+B^2=1$ and $B \geq 0$. In the same way as in Section 4.2, we can find the signed distance D between $\overline{pq}$ and v' as

$$D = A(X(v)-X(p))+B(Y(v)-Y(p)+\tfrac{H}{\tan\theta}), \tag{13}$$

where $(X(p),Y(p))$ represents the original coordinates of p.

We can also obtain the signed distance d between the edge $\overline{pq}$ and vertex v' after the optimization process, as

$$d = A(x(v)-x(p))+B(y(v)-y(p)+\tfrac{h}{\tan\theta}), \tag{14}$$

where $(x(v),y(v))$, $(x(p),y(p))$, and h are variables that correspond to the coordinates of v and p and the height of the building in the optimized map layout, respectively. Note that we can use the same values A and B in the above equation since the orientation of $\overline{pq}$ is unchanged by the fixed orientation constraints. We can notice that the road edge $\overline{pq}$ has an overlap with the shadow of the vertical building edge at v if $d>0$ as shown in Figure 6(a). Indeed, we penalize the associated occlusion by d in that case. Otherwise, the penalty is zero. In our formulation, we define this penalty cost as a new variable $\lambda(\geq 0)$ using the following constraints,

$$\lambda \geq A(x(v)-x(p))+B(y(v)-y(p)+\tfrac{h}{\tan\theta})+M, \tag{15}$$

where we take into account the same additional margin M in Section 4.2. We sum up λ for *all* the combinations of landmark road edges and basement vertices of the occluding buildings in the original layout, to compose the cost term of this first type.

As for the second type of occlusion avoidance constraint, we consider a road vertex v and its occluding building edge $\overline{pq}$, where the top corner edge of the building above $\overline{pq}$ is assumed to be projected onto the edge $\overline{p'q'}$ on the xy-plane in this case. The signed distance from $\overline{p'q'}$ to v after the optimization process amounts to

$$d = A(x(v)-x(p))+B(y(v)-y(p)-\tfrac{h}{\tan\theta}), \tag{16}$$

where $(A,B)(B>0)$ is the unit normal vector to $\overline{p'q'}$ and h is again the height of the building in the optimized layout. Now it is clear from Figure 6(b) that the vertex v is occluded by the building wall along the edge $\overline{pq}$ if $d<0$. We again formulate this occlusion as

$$\mu \geq -A(x(v)-x(p))-B(y(v)-y(p)-\tfrac{h}{\tan\theta})+M, \tag{17}$$

where we employ a new variable $\mu(\geq 0)$ to represent the amount of the associated occlusion, and penalize the overall occlusion by summing up μ for *all* the combinations of landmark road vertices and building basement edges that incur road occlusions in the original layout.

In this way, we can compose a cost function for the occlusion avoidance constraints as

$$W_o(\sum\lambda+\sum\mu), \tag{18}$$

where W_o is the weight value for penalizing undesirable occlusions of landmark roads. Note that the overall objective cost function is defined as the combination of Eqs. (11) and (18).

5 Enhancements

In this section, we also present several enhancements of our constrained optimization formulation, which include emphasizing landmark buildings, enlarging road widths for annotation, and enabling perspective projection.

5.1 Emphasizing landmark buildings

We equip our approach with the means of specifying landmark buildings such as tall buildings, historical monuments, shopping complexes, etc., so that they can visually pop up from the final optimized 3D urban maps. This is implemented by replacing Eqs. (7) and (8) with the following equations:

$$s = R_s \quad \text{and} \quad h = R_h H, \tag{19}$$

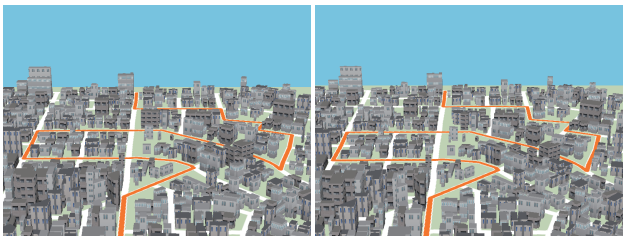

(a) (b)

Figure 7: Perspective views of a 3D urban model optimized based on (a) orthographic projection and (b) perspective projection. (Kugahara, Tokyo, Japan.)

in order to fix the sizes of the specified buildings. Here, $R_s(>1.0)$ and $R_h(>1.0)$ stand for predefined constant ratios for landmark roads and buildings, respectively, and both are set to be 1.5 by default. In addition, we drastically reduce the weight W_o in Eq. (18) specifically for the buildings so that they can still keep their enlarged sizes even when they will overlap with their surrounding roads. It is noted that we can also apply the occlusion avoidance constraints (cf. Section 4.3) to the landmark buildings and their surrounding obstacle buildings, while we provide this constraint as an option in our implementation since the above formulation can naturally enhance the visibility of the landmark buildings.

5.2 Sparing space for annotation on the roads

Annotating major roads with their names will also effectively guide travellers to identify their locations in the map. In practice, we support an operation of sparing additional space on such roads for annotation purposes. This can be archived by modifying Eq. (6) to

$$\begin{cases} A(x(v)-x(p))+B(y(v)-y(p)) \geq L-\tau & \text{if } D>0 \\ A(x(v)-x(p))+B(y(v)-y(p)) \leq -L+\tau & \text{if } D<0 \end{cases}, \tag{20}$$

where $L(\geq M)$ is the specific space additionally spared along the road. Note that τ is an error variable, which is introduced to ensure this constraint to be feasible, and expected to satisfy

$$0 \leq \tau \leq L. \tag{21}$$

The summation of τ for *all* the vertices on the roads to be annotated and their neighboring vertices, multiplied by the weight value W_r

$$W_r \sum \tau \tag{22}$$

is incorporated into the overall objective cost function in this case. As for the case when the roads have overlaps with surrounding buildings, we also replace the original margin M in Eqs. (15) and (17) with the above margin L, while we have no need to add error variables since λ and μ serve as the penalty values in this case.

5.3 Perspective projection

Suppose that we set the viewpoint to be $(0,0,T)$ and project the point $(X(v),Y(v),H)$ onto the point v' on the xy-plane, where the viewpoint is assumed to be higher than all the buildings. For realizing perspective projection, we have to update Eq. (12) as

$$(X(v'),Y(v')) = (X(v)+H\tfrac{X(v)}{T-H}, Y(v)+H\tfrac{Y(v)}{T-H}) \tag{23}$$

Nonetheless, we cannot precisely compute the coordinates of v' after the optimization process since the angle of elevation associated with v may change through the optimization. In our approach, we just approximate the position of v' by fixing the angle of elevation.

$$(x(v'),y(v')) = (x(v)+h\tfrac{X(v)}{T-H}, y(v)+h\tfrac{Y(v)}{T-H}) \tag{24}$$

This is indeed an approximated position while it yields visually plausible layout even in the case of perspective projection. Figure 7 shows how this formulation has influence on the deformation of the 3D urban map. According to the comparison between Figures 7(b) and (c), we can confirm that this new formulation can produce better occlusion-free representations of landmark routes in the perspective view.

6 Results and Discussion

This section presents several design examples obtained from real 3D urban models using our prototype system, which are followed by a user study and discussion. Our system for creating 3D urban maps has been implemented on a desktop PC with Intel Core i7-2700K (3.5GHz, 4 cores, 8MB cache) and 8GB memory. Our source code has been written in C++ using OpenGL for drawing 3D urban maps, CGAL for performing geometric computations, and IBM ILOG CPLEX for solving linear programming problems.

6.1 Design examples

Figure 1 shows a side-by-side comparison between an ordinary perspective view of a real 3D urban environment and its optimized layout obtained using our approach. The figure demonstrates that we can successfully disocclude the route (drawn in orange) while emphasizing several landmark buildings. We can also avoid occlusion of a sharply curved route even in a dense urban environment as shown in Figure 8. Our approach can extract the most feasible solution even from a difficult problem of disoccluding all the routes on the map as shown in Figure 9. Figure 10 exhibits another dense urban area where a set of specified landmark buildings successfully pop up from the final 3D map layout. We can insert additional space for annotating specific roads as shown in Figure 11. Note that in these examples we set the weight values as $W_d = 1$, $W_h = 1$, and $W_o = 50$, unless stated otherwise. Table 1 provides other statistics for these examples such as times for finding neighbor edges as a preprocess and linear programming computation, numbers of variables and linear constraints, and an angle of elevation when we look at the center of the map from the viewpoint.

The optimized layout of 3D urban maps can be adjusted by assigning different weights to the cost terms contained in the objective function. Figure 12 presents such a case where we optimize the original layout in Figure 12(a) by setting $W_d = 1, W_h = 1, W_o = 50$ to aggressively suppress the building heights as in Figure 12(b), and setting $W_d = 1, W_h = 200, W_o = 50$ to maximally retain the original heights of buildings, which eventually relaxes the horizontal displacements of geographic features as in Figure 12(c).

6.2 User study

In order to evaluate the visual readability of our 3D urban maps, we organized an eye-tracking experiment to check whether the disoccluded routes in our maps actually attract visual attention from viewers. We invited 15 participants (5 females and 10 males) working for image synthesis or cartographic design, and instructed them to visually trace the route between the blue and red landmark buildings for 5 seconds. We used the Tobii X120 eye-tracker to record the eye gaze movements of the participants. Figure 13 shows the comparison between eye-gaze distributions over the ordinary perspective view of a real 3D urban environment and its optimized version. This reveals that, in the optimized version, participants are more likely to recognize the entire layout of the landmark route. This observation suggests that our approach can make the important landmarks clearly pop up from the 3D urban maps while still providing an intuitive overview of the entire map layout.

6.3 Discussion

One of the advantages of our approach is that it can relax the local distortion of map geometry by globally optimizing the displacements of geographic features over the map domain. For example, partitioning the map domain along local seams (cf. [17, 12]) may incur unnecessary space over the entire map especially when we have to disocclude complex shaped landmark route, because the seams inevitably run out of the landmark route and thus we cannot confine the effect of the seams locally around that route. On the other hand, our approach can still provide visually plausible deformation in such cases by seeking an optimal compromise between the disocclusion of landmark features and minimal deformation in the neighborhood of the landmark route. Of course, the present formulation cannot disocclude all the specified landmarks in the case of dense urban environments while it can produce practical solutions since we penalize such undesirable occlusions by the cost function.

Table 1: Statistics for example map images. (Prep.: Times for preprocessing (in sec.), Opt.: Times for optimization (in sec.), #{Vars.}: Number of variables, #{Constrs}: Number of constraints, Angle: Angle of elevation (in deg.))

	Prep.	Opt.	#{Vars.}	#{Constrs.}	Angle
Fig. 1	1.2	3.1	12372	34057	25
Fig. 8	15.6	53.0	117724	322615	20
Fig. 9	6.7	12.7	45774	105690	20
Fig. 10	2.4	6.9	22363	59067	20
Fig. 11	2.7	8.4	25490	66550	30

Our formulation is still limited to static cases where the map domain is explicitly segmented from the entire geographic data to leave enough degrees of freedom in the map deformation. Indeed, this is helpful for our approach because we are more likely to keep our constrained optimization problems to be feasible even in dense urban environments. Nonetheless, our framework has been carefully designed and thus we never encountered infeasible problems and hardly ever saw unnatural map distortions in our experiments. Furthermore, we have another option of tweaking the weight values assigned to the individual cost terms to alleviate unexpected visual artifacts. Our experience suggests that we can still improve such unusual cases by decreasing W_o in Eq. (18) to relax the occlusion avoidance constraints for more flexibility in map deformation.

7 Conclusion

This paper has presented an approach for automatically creating 3D urban maps where the occlusions of important landmarks are successfully eliminated through the deformation of its geographic layout. This has been accomplished by formulating the constrained optimization problem for minimizing the geographic deformation while satisfying the design criteria derived from hand-drawn illustrative maps. The linear programming techniques are effectively introduced to automatically generate the occlusion-free representation of important landmarks specified by users. Design examples together with results of our user study demonstrated that our approach considerably improves the visual readability of the 3D urban maps according to the users' preferences.

In our future work, we plan to extend the present framework to mixed-integer programming formulations [16] so that we can also incorporate either-or constraints (i.e. the union of convex solution regions). Handling complicated objects such as non-prism shaped buildings and arch-like structures over roads may further enhance the reality of the 3D urban maps. Sophisticated annotation techniques can help us further alleviate the problem of avoiding occlusions of important landmark features in 3D urban maps. More formal user studies should be conducted to assess the advantages of our maps in various real urban environments. Our future extensions also include animating the occlusion-free representation of 3D urban maps for effectively guiding users to drive their vehicles in urban areas.

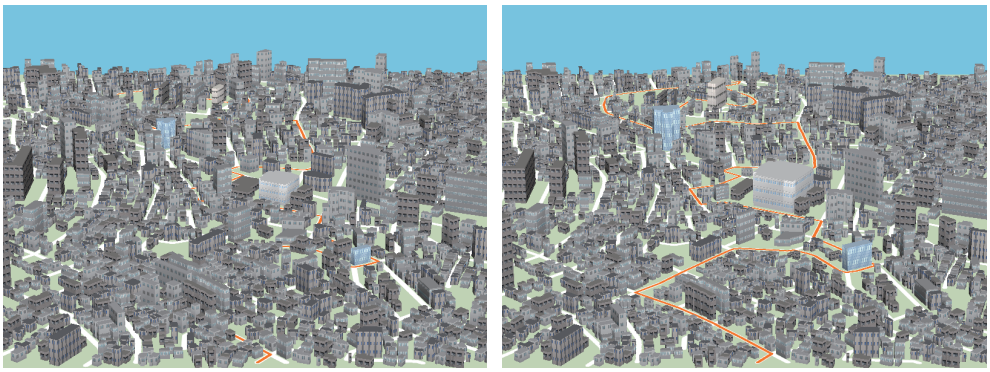

Figure 8: A complicated 3D urban environment where a sharply curved route is disoccluded. An ordinary perspective image (left) and its optimized version (right). (Suwazaka, Yokohama, Japan.)

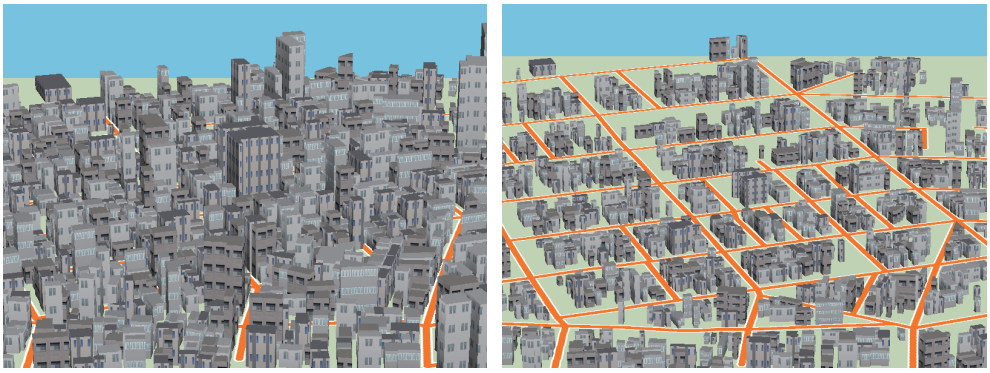

Figure 9: An optimized layout of a 3D urban map where all the routes are selected as landmarks. An ordinary perspective image (left) and its optimized version (right). (Nishi-Kamata, Tokyo, Japan.)

Figure 10: An optimized layout of a 3D urban map while landmark buildings are emphasized. An ordinary perspective image (left) and its optimized version (right). (Okurayama, Yokohama, Japan.)

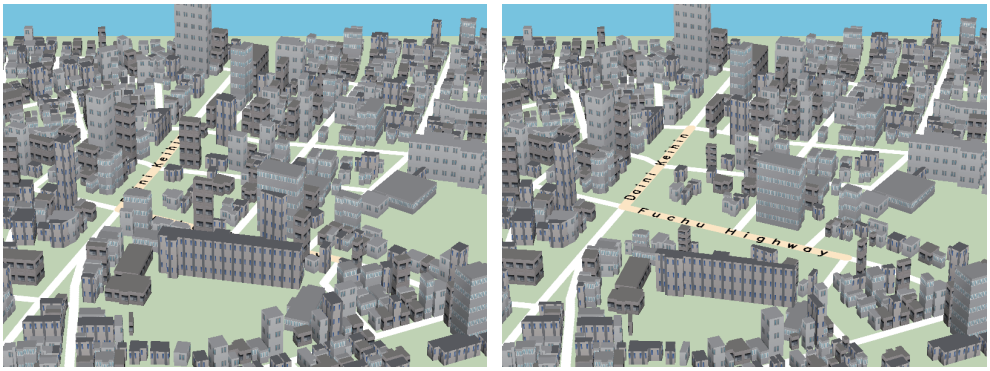

Figure 11: Additional space for annotating roads has been introduced into a 3D urban map. An ordinary perspective image (left) and its optimized version (right). Note that we set $W_r = 50$ in this case. (Endo-machi, Kawasaki, Japan.)

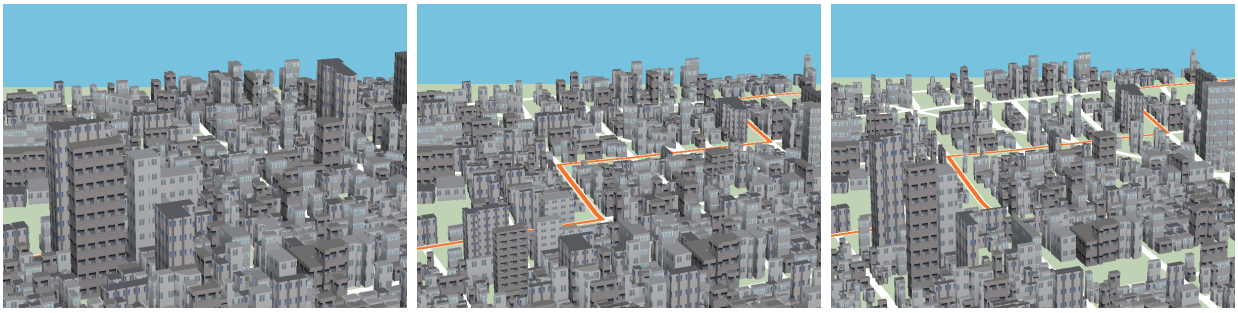

(a) (b) (c)

Figure 12: Optimized 3D urban layouts with different weight assignments. (a) An ordinary perspective image. Disoccluding the landmark route when (b) $W_d = 1, W_h = 1, W_o = 50$ and (c) $W_d = 1, W_h = 200, W_o = 50$. The angle of elevation is 20 degrees in this case. (Asada, Kawasaki, Japan.)

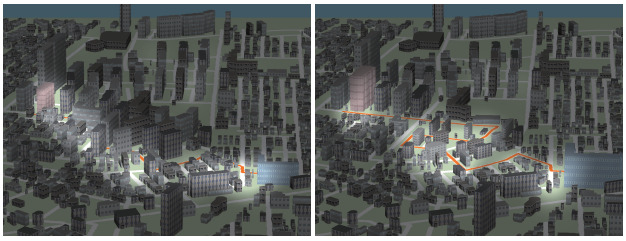

(a) (b)

Figure 13: Comparisons between eye-gaze distributions between the (a) ordinary perspective view and (b) its optimized layout where a landmark route is disoccluded. The image opacity is reduced according to the length of the eye-gaze fixation time. (Matsubacho, Chiba, Japan.)

Acknowledgments

The authors would like to thank anonymous reviewers for their helpful comments. The hand-drawn map in Figure 2 is courtesy of WORKS-PRESS CO., LTD. 3D urban models of Japan provided by ZENRIN CO., LTD and digital road map databases of Japan provided by Sumitomo Electric Industries, Ltd are used as the joint research (No. 398) using spatial data provided by Center for Spatial Information Science, the University of Tokyo. This work has been partially supported by JSPS under Grants-in-Aid for Scientific Research (B) No. 24330033.

References

[1] M. Agrawala and C. Stolte. Rendering effective route maps: Improving usability through genralization. In *Proceedings of ACM SIGGRAPH 2001*, pages 241–250, 2001.

[2] S. Carpendale, J. Light, and E. Pattison. Achieving higher magnification in context. In *Proceedings of the ACM Symposium on User Interface Software and Technology*, pages 71–80, 2004.

[3] A. Chaudhuri and H.-W. Shen. A self-adaptive techniques for visualizing geospatial data in 3D with minimum occlusion. In *Proceedings of Visualization and Data Analysis 2012*, volume 8294, 2012.

[4] M. Christie, P. Olivier, and J.-M. Normand. Camera control in computer graphics. *Computer Graphics Forum*, 27(8):2197–2218, 2008.

[5] J. Cui, P. Rosen, V. Popescu, and C. Hoffmann. A curved ray camera for handling occlusions through continuous multiperspective visualization. *IEEE Transactions on Visualization and Computer Graphics*, 16(6):1235–1242, 2010.

[6] P. Degener and R. Klein. A variational approach for automatic generation of panoramic maps. *ACM Transactions on Graphics*, 28(1), 2009. Article No. 2.

[7] N. Elmqvist and P. Tsigas. A taxonomy of 3D occlusion management for visualization. *IEEE Transactions on Visualization and Computer Graphics*, 14(5):1095–1109, 2008.

[8] F. Grabler, M. Agrawala, R. W. Sumner, and M. Pauly. Automatic generation of tourist maps. *ACM Transactions on Graphics*, 27(3), 2008. Article No. 100.

[9] J.-H. Haunert and L. Sering. Drawing road networks with focus regions. *IEEE Transactions on Visualization and Computer Graphics*, 17(12):2555–2562, 2011.

[10] J. Kopf, M. Agrawala, D. Bargeron, D. Salesin, and M. Cohen. Automatic generation of destination maps. *ACM Transactions on Grahics*, 29(6), 2010. Article No. 158.

[11] Y. K. Leung and M. D. Apperley. A review and taxonomy of distortion-oriented presentation techniques. *ACM Transactions on Computer-Human Interaction*, 1(2):126–160, 1994.

[12] Z. Liqiang, D. Hao, C. Dong, and W. Zhen. A spatial cognition-based urban building clustering approach and its applications. *International Journal of Geographical Information Science*, 2012. to appear.

[13] M. Lonergan and C. B. Jones. An interactive displacement method for conflict resolution in map generation. *Algorithmica*, 30:287–301, 2001.

[14] A. M. MacEachren. *How Maps Work*. The Guilford Press, 1995.

[15] S. Möser, P. Degener, R. Wahl, and R. Klein. Context aware terrain visualization for wayfinding and navigation. *Computer Graphics Forum*, 27(7):1853–1860, 2008.

[16] M. Nöllenburg and A. Wolff. Drawing and labeling high-quality metro maps by mixed-integer programming. *IEEE Transactions on Visualization and Computer Graphics*, 17(5):626–641, 2011.

[17] H. Qu, H. Wang, W. Cui, Y. Wu, and M.-Y. Chan. Focus+Context route zooming and information overlay in 3D urban environments. *IEEE Transactions on Visualization and Computer Graphics*, 15(6):1547–1554, 2009.

[18] A. Semmo, M. Trapp, J. E. Kypianidis, and J. Döllner. Interactive visualization of generalized virtual 3D city models using level-of-abstraction transitions. *Computer Graphics Forum*, 31(3):885–894, 2012.

[19] S. Takahashi, K. Yoshida, K. Shimada, and T. Nishita. Occlusion-free animation of driving routes for car navigation systems. *IEEE Transactions on Visualization and Computer Graphics*, 12(5):1141–1148, 2006.

[20] R. Tamassia. Constraints in graph drawing algorithms. *Constraints*, 3(1):87–120, 1998.

[21] M. Trapp, T. Glander, H. Buchholz, and J. Döllner. 3D generalization lenses for interactive Focus+Context visualization of virtual city models. In *Proceedings of the 12th International Conference on Information Visualization*, pages 356–361, 2008.

[22] Y.-S. Wang and M.-T. Chi. Focus+Context metro maps. *IEEE Transactions on Visualization and Computer Graphics*, 17(12):2528–2535, 2011.

[23] Y.-S. Wang, T.-Y. Lee, and C.-L. Tai. Focus+Context visualization with distortion minimization. *IEEE Transactions on Visualization and Computer Graphics*, 14(6):1731–1738, 2008.

[24] H. Zhou, X. Yuan, H. Qu, W. Cui, and B. Chen. Visual clustering in parallel coordinates. *Computer Graphics Forum*, 27(3):1047–1054, 2008.